

EGG-M--10087

DE89 011159

Received by OSTI

MAY 08 1989

ULTRASONIC CHARACTERIZATION OF POROSITY IN ADVANCED SiC CERAMIC COMPOSITES

J. B. Walter and L. A. Lott
Idaho National Engineering Laboratory
EG&G Idaho, Inc.
Idaho Falls, ID 83415

Paul M. Gammell
Naval Surface Weapons Center
Silver Spring, MD 20903-5000

INTRODUCTION

Ceramic reinforced ceramic matrix composites are advanced materials currently being developed for high temperature, high strength applications such as heat engine components, heat exchangers and recuperators.

The particular material considered here was SiC fiber reinforced SiC matrix formed by chemical vapor infiltration (CVI). The initial focus was on porosity, which has been linked to the material strength.¹ Ultrasonic attenuation and velocity were investigated since they were expected to be affected by the porosity in the material.^{2,3,4}

The objectives of the study were to determine the capability of conventional methods to measure the ultrasonic properties of the materials, and develop improved methods where necessary; to determine the correlations between ultrasonic properties and material properties of interest; and to demonstrate the ability of the ultrasonic technique to nondestructively characterize ceramic composite components.

EXPERIMENTAL METHODS

A set of SiC/SiC samples designed to have a wide range of porosity levels was used in this study. The samples were in the form of plates measuring approximately 100 x 38 x 3.3 mm. They were fabricated from preforms built up from multiple layers of SiC cloth^a. The SiC matrix was added by a chemical vapor infiltration (CVI) process.^b The process results in samples with high porosity because, as matrix continues to deposit on the fibers in the preform, further infiltration of the gaseous reactants can be inhibited. The bulk porosity varied between 26-42 volume percent for the samples examined.

^a Nicalon, Nippon Carbon Co., Tokyo, Japan.

^b Refractory Composites, Inc., Whittier, California.

DISCLAIMER

This report was prepared as an account of work sponsored by an agency of the United States Government. Neither the United States Government nor any agency thereof, nor any of their employees, makes any warranty, express or implied, or assumes any legal liability or responsibility for the accuracy, completeness, or usefulness of any information, apparatus, product, or process disclosed, or represents that its use would not infringe privately owned rights. Reference herein to any specific commercial product, process, or service by trade name, trademark, manufacturer, or otherwise does not necessarily constitute or imply its endorsement, recommendation, or favoring by the United States Government or any agency thereof. The views and opinions of authors expressed herein do not necessarily state or reflect those of the United States Government or any agency thereof.

DISCLAIMER

Portions of this document may be illegible in electronic image products. Images are produced from the best available original document.

Because the ultrasonic attenuation of these 3mm thick specimens was extremely high (typically 50 to 80 db at 2.5 MHz), studies were limited to through-transmission measurements. Some ultrasonic measurements were performed using a standard two transducer transmission system with 2.25 MHz 12.7 dia. piezoelectric transducers. The samples were immersed directly in the water tank. Since thicker specimens may be studied in the future and since reflected ultrasound may be desired either for measurement of the depth of defects or for single-sided inspection, two techniques with great potential for improving the ultrasonic sensitivity were investigated.

One of the techniques of sensitivity improvement is laser-generated ultrasound. The sample was placed at the surface of the water tank and a laser pulse of about 10 ns, 5 mJ was directed in an approximately 6 mm diameter spot on the surface of the specimen that was above the water. The sound wave generated by thermoelastic conversion propagated through the sample to the immersed surface and was received by an ordinary piezoelectric transducer located about 12 mm from the sample in the water. Both the ultrasonic propagation velocity and the amount of ultrasonic energy transmitted through the sample were measured. This technique provided 20 to 30 dB more signal at the receiver than was available when a piezoelectric transmitter was used. A more complete description of the technique is given in reference 5.

The other technique of sensitivity improvement uses a unique type of averaging, rather than higher power levels, for signal-to-noise improvement. This technique, time delay spectrometry (TDS) uses the unique properties of a linearly swept frequency signal to provide rapid signal averaging and can obtain an improvement equivalent to averaging thousands of pulse-echo signals in only 20 ms. When the swept frequency is received after propagation through the sample (and possibly other paths) components of different propagation delays are distinguished by their frequency offset relative to the linear transmitted sweep. If the received signal is heterodyned against the transmitted sweep, the lower sideband represents a signal in which the known linear sweep is subtracted. For a fixed frequency in this signal, the frequency of the ultrasonic signal is represented by the time since the start of the sweep, while for a fixed arrival time, the time delays of the components are represented by their frequencies. Simple fixed filters can be used to select signals arriving within some bandwidth of the linear sweep, resulting in a signal-to-noise improvement over pulsed operation equal to the ratio of the ultrasonic bandwidth of the sweep to the bandwidth of the filter. This ratio is typically 20 MHz/1KHz (43 dB).

Since this processing preserves phase information, the time domain representation (ultrasonic A-scan) can be recovered using a simple Fast Fourier Transform (FFT), with an even greater signal-to-noise improvement.^{6,7} TDS has also been used in the reflection mode with a single transducer.⁸

RESULTS AND DISCUSSION

Figures 1 and 2 show the measured correlations between the porosity and the attenuation and velocity, respectively, using conventional piezoelectric transducers in the throughtransmission mode. Each error bar is the standard deviation of the measurements for the corresponding sample, and is indicative of the degree of uniformity. The lines through the data are the result of unweighted least squares analyses, and give changes per percent porosity of 0.5 dB/mm for attenuation (at 1.6 MHz) and 0.16 km/s for velocity.

Ultrasonic maps of a sample reveal nonuniform distributions of porosity. A sample having large variations in porosity is featured in Figure 3. The X-ray radiograph in Figure 3a, which was calibrated by a series of penetrameters, reveals that the porosity ranges from as low as 27% in the dark region to as high as 35% in the light region. The ultrasonic maps show the same general pattern as does the radiograph; three areas of relatively high material density surrounded by areas of higher porosity. The lower porosity regions transmit more energy, and have higher velocity. The range of velocities in Figure 3c, about 3.5 to 5.5 km/s, is consistent with the velocity measurements in Figure 2.

Figure 4 shows the attenuation spectra at three locations of the same sample obtained with the TDS technique. The two upper spectra were taken at regions of high porosity in the sample and the lower spectrum was taken at the central low porosity region. These show the measured trend of increasing attenuation with increasing frequency and higher attenuation associated with higher material porosity. The extremely high attenuation levels in the material are evident. Materials with such high attenuation levels would be extremely difficult if not impossible to examine with conventional pulsed ultrasonic techniques. The sharp cusps seen in the spectra are associated with phase cancellation effects at the transducer face caused by velocity variations in the sample.

CONCLUSIONS

The density of these developmental specimens varies considerably, both between samples and within a given sample. Radiography, ultrasonic velocity maps, and ultrasonic attenuation maps are in general agreement as to the high and low density areas. When compared to the average sample density the ultrasonic velocity shows a strong positive correlation and the ultrasonic attenuation shows a fair negative correlation. The signs of these correlations are as expected from simple considerations. If comparison were made between these ultrasonic properties and the local sample density, better correlations are expected, although the ultrasonic properties are expected to depend on the contact between sample components as well as on the local density.

Because of the high attenuation of these samples, if thicker samples are to be inspected or if reflection methods are to be used, the signal-to-noise improvement of techniques such as TDS and/or the laser generation method will be needed.

ACKNOWLEDGMENTS

This work was supported by the U.S. Department of Energy Assistant Secretary for Fossil Energy, Office of Technology Coordination, under DOE Contract No. DE-AC07-76ID01570 and by the Materials Block Program and the Internal Exploratory Development Program at the Naval Surface Weapons Center.

REFERENCES

1. A. J. Caputo, D. P. Stinton, R. A. Lowden, and T. M. Bessmann, "Fiber-Reinforced SiC Composites with Improved Mechanical Properties," *Am. Ceram. Soc. Bull.* 66, 368 (1987).
2. J. H. Rose, "The Effect of Nonspherical Pores and Multiple Scattering on the Ultrasonic Characterization of Porosity," in *Review of Progress in Quantitative Nondestructive Evaluation*, Vol. 6B, D. O. Thompson and D. E. Chimenti, Eds., Plenum Publishing Corporation (1987).
3. S. J. Klima, "NDE of Advanced Ceramics," *Materials Evaluation*, 44, 571 (1986).
4. S. W. Wang, A. Csankany, L. Adler, and C. Mobley, "Ultrasonic Determination of Porosity in Cast Aluminum," in *Review of Progress in Quantitative Nondestructive Evaluation*, Vol. 4B, D. O. Thompson and D. E. Chimenti, Eds., Plenum Publishing Corporation (1985).
5. J. B. Walter, L. A. Lott and K. L. Telschow, "Ultrasonic Characterization of Ceramic-Ceramic Composites," *Proceedings of the Review of Progress in QNDE*, I, Plenum Press, 1988 (to be published)
6. P. M. Gammell, "Ultrasonic Characterization of Highly Attenuating Materials with Time Delay Spectrometry," *Proceedings of the 15th Symposium on Nondestructive Evaluation*, 23-25 April, 1985, San Antonio, TX (1986) (available NTIAC, San Antonio, TX), pp. 292-302.
7. P. M. Gammell, "Time and Frequency Domain Measurements of Materials with High Attenuation Using Time Domain Spectroscopy", *Review of Progress in Quantitative NDE*, Vol. 5, D. O. Thompson and D. E. Chimenti, Eds., Plenum Press, (1986) pp. 759-765.
8. P. M. Gammell, "Single Transducer Swept Frequency Ultrasonic Reflection Measurements," *Ultrasonics* 17, 183-185 (1979)

FIGURE CAPTIONS

Figure 1. Attenuation at 1.6 MHz as a function of sample porosity. The attenuation increases at about 0.5 dB/% porosity. The error bars are the standard deviation values measured at different points on the sample. Two sets of measurements are shown for two of the samples.

Figure 2. Acoustic velocity measured with the conventional pulsed system. Velocity is seen to depend strongly on the sample porosity. The error bars are the standard deviation of measurements at different points on the sample. Two sets of measurements are shown for one sample.

Figure 3. SiC-SiC sample with porosity variations from 28% to 35%. a) Positive print of X-ray radiograph, and maps of b) the transmitted ultrasonic energy (darker = higher energy), and c) the ultrasonic propagation velocity (darker = higher velocity).

Figure 4. Ultrasonic attenuation measured with TDS technique for the SiC-SiC sample in Figure 3, at the central low porosity region and in the higher porosity regions on either side.

Ultrasonic Attenuation Correlates with Porosity for SiC-SiC Samples

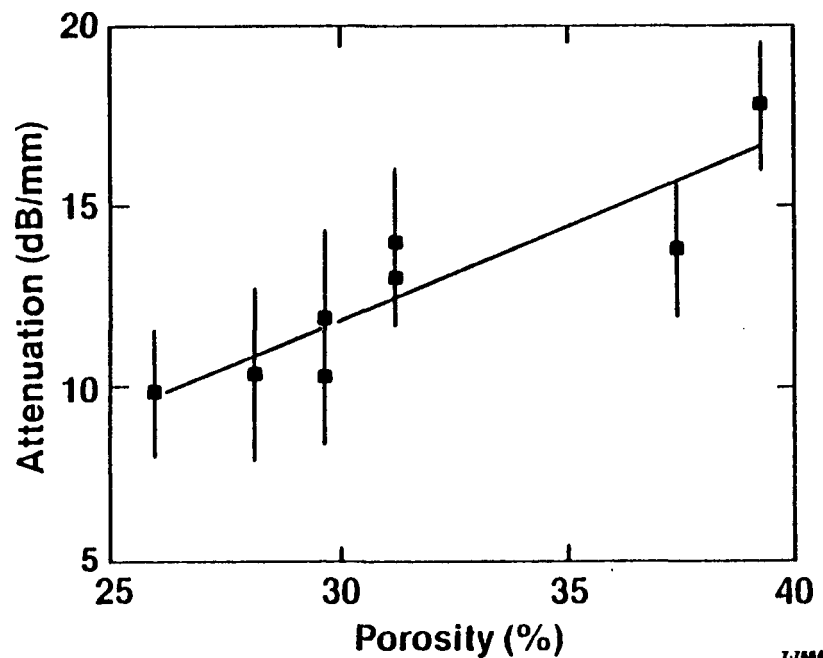


Figure 1

Ultrasonic Velocity Correlates with Porosity for SiC-SiC Samples

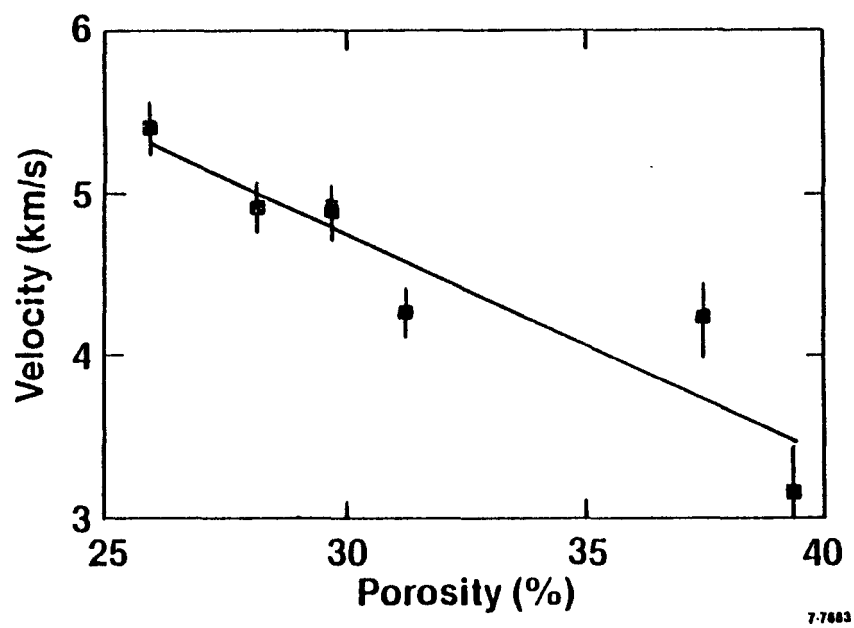


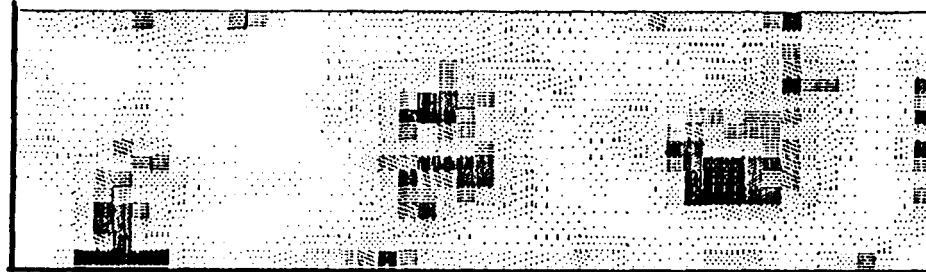
Figure 2



Figure 3a

Transmitted Energy

RCI 238



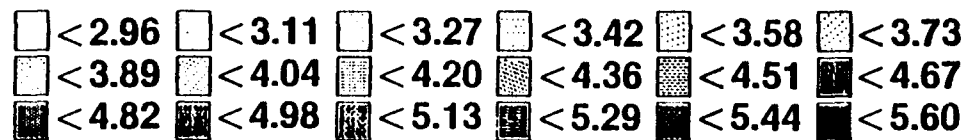
□ < 88.89 □ < 177.78 □ < 266.67 □ < 355.56 □ < 444.44 □ < 533.33
□ < 622.22 □ < 711.11 □ < 800.00 □ < 888.89 □ < 977.78 □ < 1066.67
□ < 1155.56 □ < 1244.44 □ < 1333.33 □ < 1422.22 □ < 1511.11 □ < 1600.00

7-10168

Figure 3b.

Velocity

RCI 238



7-10173

Figure 3c.

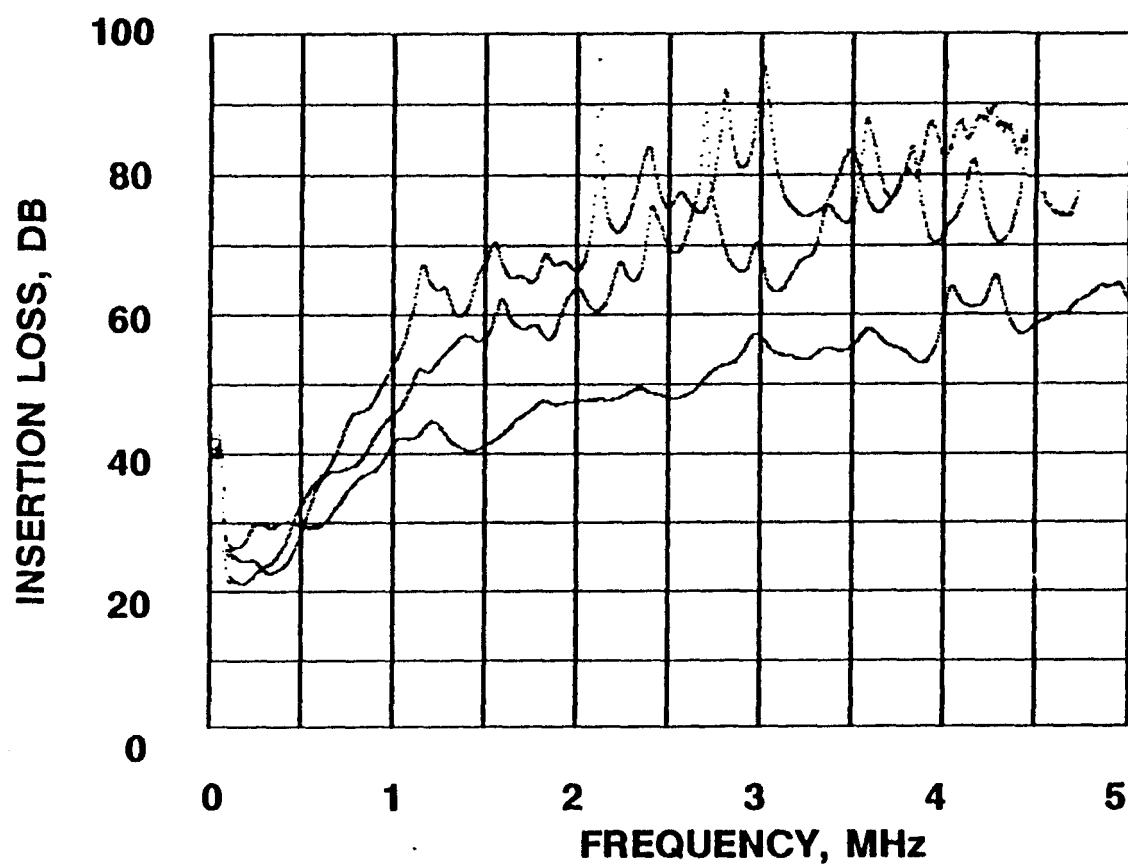


Figure 4

ATTENUATION SPECTRA
AT LOCATIONS MARKED
ON IMAGE

DATA: 27JUL87A ART/WP: SP105